Int. Conference on Boundary and Interior Layers
BAIL 2006
G. Lube, G. Rapin (Eds)
© University of Göttingen, Germany, 2006

Convection-diffusion problems, SDFEM/SUPG and a priori meshes

Martin Stynes

Mathematics Department, National University of Ireland, Cork, Ireland
m.stynes@ucc.ie

1. Introduction and summary

This paper aims to give the reader a summary of current understanding of the streamline-diffusion finite element method (SDFEM), as applied to linear steady-state convection-diffusion problems. Towards this end, we begin with a brief description of the nature of convection-diffusion problems: the structure of their solutions will be examined, with special emphasis on the main phenomena of exponential and characteristic/parabolic layers. See [34] for a more leisurely and detailed exposition of this material.

Next, Shishkin meshes will be presented and discussed. These piecewise-uniform meshes are suited to the numerical solution of convection-diffusion problems with boundary layers. Further information on them appears in [7, 27, 30, 31, 34].

Finally, we come to the Streamline Diffusion Finite Element Method (SDFEM), which is also known as the Streamline-Upwinded Petrov-Galerkin method (SUPG). Since its inception [12] in 1979, this method has been the subject of a huge number of theoretical analyses and numerical investigations that continue to this day; see the references in [30, 31, 34]. We shall give a comprehensive survey of the application of the method to convection-diffusion problems, including discussions of its strengths and weaknesses, and present recent theoretical results.

2. Convection-diffusion problems

Steady-state convection-diffusion problems are boundary value problems of the form

$$-\varepsilon\Delta u + \mathbf{a}\cdot\nabla u = f \text{ on } \Omega, \qquad u = g \text{ on } \partial\Omega \tag{1}$$

where Ω is some domain in R^n with boundary $\partial\Omega$; for simplicity we have taken Dirichlet boundary conditions. Here ε is a small positive parameter, so the second-order differential operator is elliptic — but the smallness of ε means that the ellipticity constant is close to zero, which gives reduced stability for standard numerical methods.

The term $-\varepsilon\Delta u$ models diffusion while $\mathbf{a}\cdot\nabla u$ models convection. The terminology *convection-diffusion problem* is used since the convection coefficient has much greater magnitude than the diffusion coefficient:

$$\frac{|\text{coefficient of } \nabla u|}{|\text{coefficient of } \Delta u|} = \frac{|\mathbf{a}|}{\varepsilon} \gg 1.$$

For almost all boundary conditions this is an example of a singularly perturbed problem: the solution in the case $\varepsilon = 0$ is not equal at all points to the limit of the solution as $\varepsilon \to 0$.

Applications of convection-diffusion problems include the linearized Navier-Stokes equations (the Oseen equations) and the drift-diffusion equation of semiconductor device modelling; Morton [28] gives further examples.

We shall consider only problems posed in two-dimensional domains Ω. Writing $\mathbf{n}$ for the outward-pointing unit normal to boundary $\partial\Omega$, we divide it into three parts (see Figure 1):

$$\text{inflow boundary } \partial^-\Omega = \{x \in \partial\Omega : \mathbf{a}\cdot\mathbf{n} < 0\}$$
$$\text{outflow boundary } \partial^+\Omega = \{x \in \partial\Omega : \mathbf{a}\cdot\mathbf{n} > 0\}$$
$$\text{tangential/characteristic flow boundary } \partial^0\Omega = \{x \in \partial\Omega : \mathbf{a}\cdot\mathbf{n} = 0\}$$

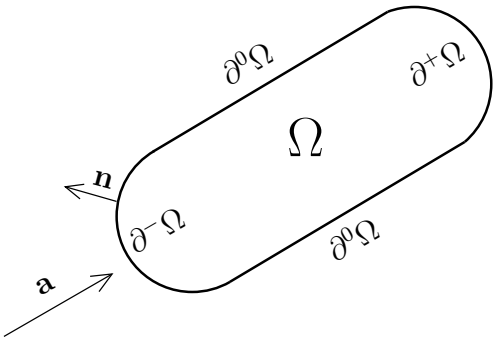

Figure 1: Partition of $\partial\Omega$

Then the solution u of (1) has the following asymptotic structure:

$$u = \text{reduced solution} + \text{layers} + \text{negligible terms} \tag{2}$$

Here the "reduced solution" is the solution u_0 of the first-order partial differential equation $\mathbf{a}\cdot\nabla u_0 = f$ on Ω, which is obtained by formally setting $\varepsilon = 0$ in (1), with the boundary data $u_0 = g$ on $\partial^-\Omega$. The "layers" are narrow regions where u changes rapidly, so certain derivatives of u are consequently large there. Along $\partial^+\Omega$ the solution usually has an *exponential boundary layer* — this can be written in terms of exponential functions — and along $\partial^0\Omega$ the solution typically has *parabolic* or *characteristic boundary layers*, which are so called because (i) they are often expressed as the solutions of associated parabolic partial differential equations and (ii) these layers lie along the characteristic traces of the operator $\mathbf{a}\cdot\nabla$.

Example 1

$$-\varepsilon\Delta u(x,y) + u_x(x,y) = 1 \text{ on } \Omega := (0,1)\times(0,1), \qquad u(x,y) \equiv 0 \text{ on } \partial\Omega.$$

The inflow boundary is the side $x = 0$ of $\bar{\Omega}$. The reduced solution is $u_0(x,y) = x$. One has $u \approx u_0$ away from the outflow boundary $x = 1$ (where there is an exponential layer) and the characteristic boundaries $y = 0$ and $y = 1$ (where there are characteristic layers). See Figure 2. for a computed solution.

Layers away from boundaries — *(characteristic) interior layers* — are also possible:

Example 2 *Consider again the differential equation*

$$-\varepsilon\Delta u(x,y) + u_x(x,y) = 1 \quad \text{on } \Omega := (0,1)\times(0,1),$$

with now a jump discontinuity in the boundary data on $\partial^-\Omega$. This induces an interior layer in the solution u. The boundary data along $y = 0$ and $y = 1$ have been chosen to agree with u_0 so that no characteristic boundary layers are visible. An exponential layer is still present at $\partial^+\Omega$. See Figure 3 for a computed solution.

When two glaciers meet, an interior layer in the ice is formed naturally by transported sediment and is called a medial moraine. See Figure 4 for an example taken from [19].

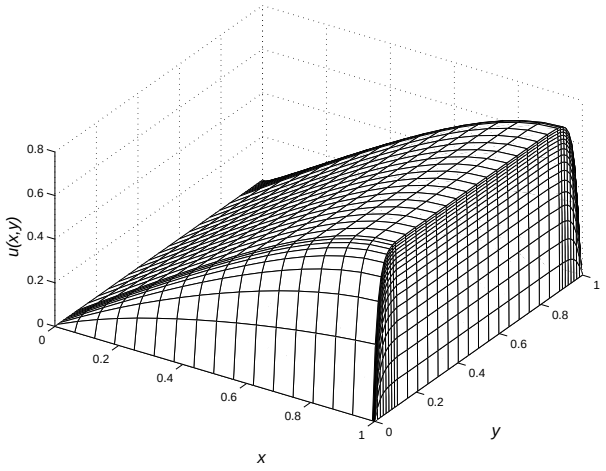

Figure 2: Solution to Example 1

3. Shishkin meshes

One-dimensional Shishkin meshes are piecewise equidistant meshes: first partition the domain (an interval) into two subintervals of very unequal length by a "transition point", then use half the mesh intervals to subdivide each of these subintervals equidistantly, resulting in a mesh that contains equal numbers of fine and coarse mesh intervals, with the fine and coarse intervals meeting only at the transition point. Shishkin meshes on two-dimensional rectangular domains are tensor products of one-dimensional Shishkin meshes.

Suppose that we wish to solve the problem

$$-\varepsilon\Delta u + a_1 u_x + a_2 u_y = f \text{ on } \Omega := (0,1)\times(0,1), \quad \text{with } a_1 > 0, a_2 > 0.$$

Then the solution u has exponential boundary layers along $x = 1$ and $y = 1$; see Section 2.. For this problem, the rectangular (and triangular — obtained by dividing each rectangle into two triangles) Shishkin meshes are given in Figure 5. Here the *transition points* $1-\sigma_x$ and $1-\sigma_y$ that separate the coarse and fine meshes in each coordinate direction are defined using $\sigma_x = (k/\beta_1)\varepsilon \ln N$, $\sigma_y = (k/\beta_2)\varepsilon \ln N$, where $\beta_i = \min_{(x,y)\in\bar{\Omega}} a_i(x,y)$ and k is a user-chosen parameter; typically k is approximately equal to the order of convergence expected of the method.

If instead we consider the problem $-\varepsilon\Delta u - a_1 u_x = f$, with $0 < \beta_1 = \min_{(x,y)\in\bar{\Omega}} a_1(x,y)$, on the unit square Ω, then the solution has an exponential boundary layer at $x = 0$ and parabolic boundary layers at $y = 0, 1$. The appropriate Shishkin mesh with $\sigma_x = (k/\beta_1)\varepsilon \ln N$, $\sigma_y = k\sqrt{\varepsilon}\ln N$ is shown in Figure 6; once again, half the mesh intervals lie in the coarse mesh in each coordinate direction.

An approximate Shishkin mesh is constructed in [26] to generate a numerical solution for a problem on the unit square that has a curved interior layer lying along a quarter-circle; the symmetric shape of the layer's location aids in the mesh construction.

Many examples of Shishkin meshes on rectangular domains appear in the literature, but I can find no published numerical example for a convection-diffusion problem where a Shishkin mesh is implemented on a domain with curved boundary. (There are such examples for reaction-diffusion problems; see e.g. [18].) The photograph in Figure 7 illustrates how a Shishkin mesh

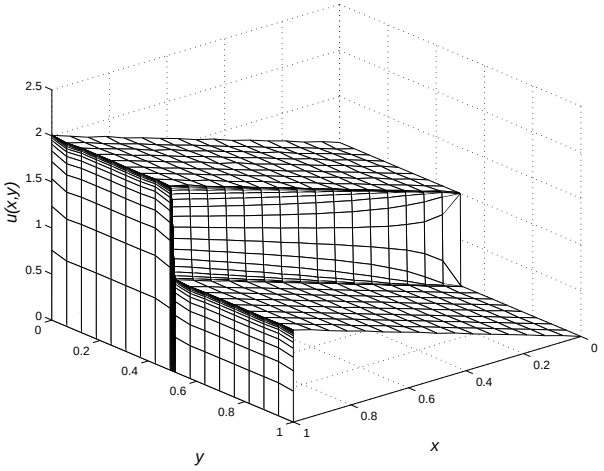

Figure 3: Solution to Example 2; characteristic interior layer

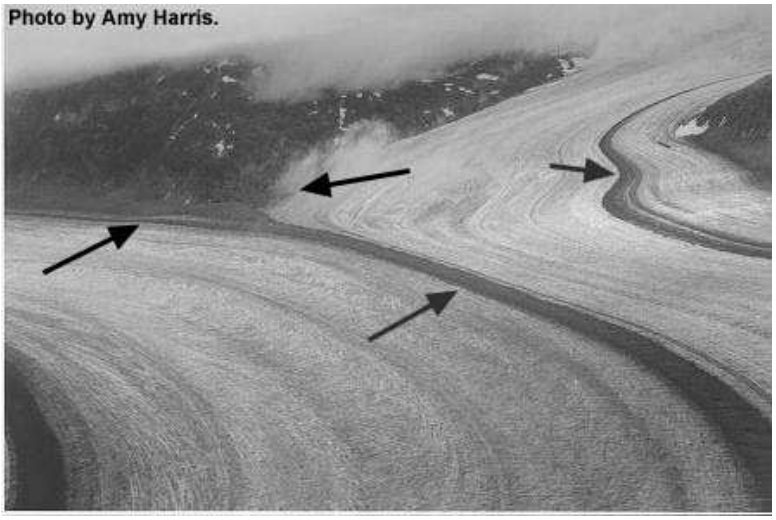

Figure 4: Medial moraines (two rightmost arrows) start where two glaciers meet

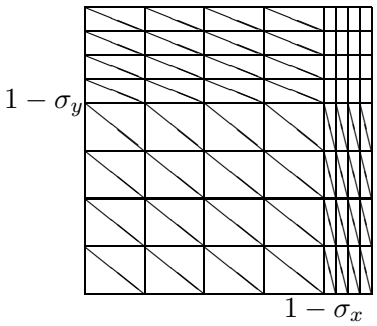

Figure 5: Tensor product Shishkin mesh; layers at $x = 1$ and $y = 1$

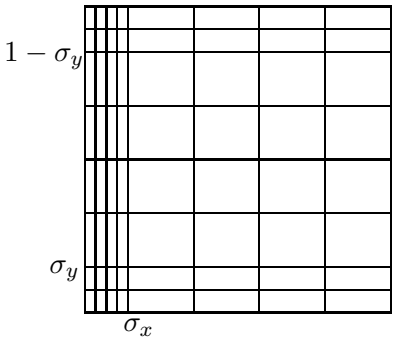

Figure 6: Shishkin mesh; layers at $x = 0,\ y = 0$ and $y = 1$

should look at a curved boundary: it is very fine in the direction perpendicular to the boundary until it reaches a predetermined distance from the boundary, where it can become an arbitrary coarse mesh.

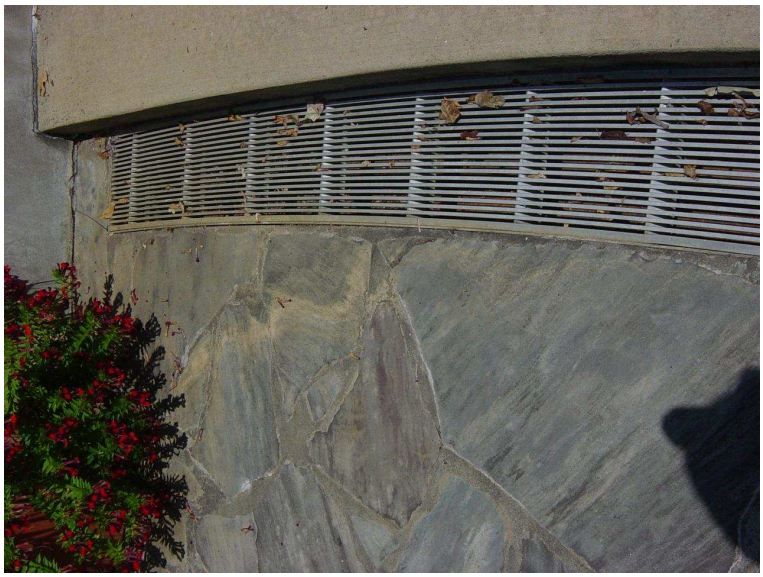

Figure 7: "Shishkin mesh" at curved boundary

Other layer-adapted meshes are used by some authors. In particular the Bakhvalov mesh for convection-diffusion problems is graded and does not have the abrupt transition from fine to coarse that appears in the Shishkin mesh, but it is more troublesome to construct. Linß [21, 22] gives excellent surveys of layer-adapted meshes for convection-diffusion problems.

4. SDFEM/SUPG

Throughout the rest of the paper we consider the boundary value problem

$$-\varepsilon\Delta u + \mathbf{a}\cdot\nabla u + cu = f \quad \text{on } \Omega \subset R^2, \tag{3a}$$

$$u = 0 \quad \text{on } \partial\Omega, \tag{3b}$$

with $0 < \varepsilon \ll 1$. Make the usual finite element assumption that $c - \operatorname{div} \mathbf{a}/2 \geq c_0 > 0$ on $\bar{\Omega}$ for some c_0.

Let $\mathcal{T}_h$ be a triangulation of Ω. For simplicity here we confine our attention to the case where $\mathcal{T}_h$ comprises triangles or rectangles with no hanging nodes, but some of the subsequent analysis also applies to more general subdivisions of Ω. On this triangulation we use a standard conforming piecewise polynomial trial space $V^N \subset H_0^1(\Omega)$. (A nonconforming variant of the SDFEM is analysed in [16].)

Notation. C will denote a generic constant that is independent of ε and of the mesh.

The standard Galerkin FEM for (3) is: find $u^N \in V^N$ such that for all $v \in V^N$,

$$\begin{aligned} a_{Gal}(u^N, v^N) &:= \varepsilon(\nabla u^N, \nabla v^N) + (\mathbf{a} \cdot \nabla u^N, v^N) + (cu^N, v^N) \\ &= (f, v^N), \end{aligned}$$

where $(\cdot, \cdot)$ is the $L^2(\Omega)$ inner product.

How stable is this method? For all $v^N \in V^N$, since $V^N \subset H_0^1(\Omega)$ we get

$$\begin{aligned} a_{Gal}(v^N, v^N) &= \varepsilon(\nabla v^N, \nabla v^N) + (\mathbf{a} \cdot \nabla v^N, v^N) + (cv^N, v^N) \\ &= \varepsilon |v^N|_1^2 + \left(c - \frac{1}{2} \operatorname{div} \mathbf{a}, (v^N)^2 \right) \\ &\geq \varepsilon |v^N|_1^2 + c_0 \|v^N\|_0^2 \\ &=: \|v^N\|_{1,\varepsilon}^2. \end{aligned} \tag{4}$$

Here $|\cdot|_1$ is the $H^1(\Omega)$ seminorm and $\|\cdot\|_0$ denotes the $L^2(\Omega)$ norm.

The stability implied by the coercivity inequality (4) is much weaker than the stability enjoyed by the same method in the classical case $\varepsilon = 1$ because $\|\cdot\|_{1,\varepsilon}$ is a weak norm compared with the standard $H^1(\Omega)$ norm $\|\cdot\|_1$. The numerical example of Figure 8 shows this only too well: the computed solution is plagued by wild oscillations and the true solution cannot be discerned.

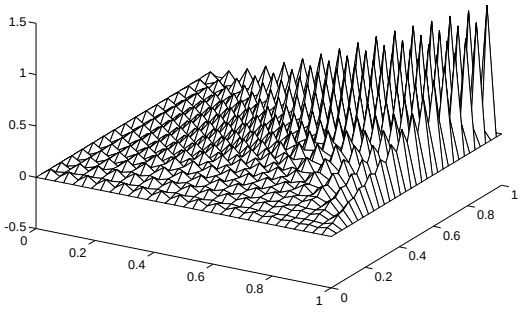

Figure 8: Galerkin FEM on equidistant mesh, $\varepsilon = 10^{-3}$

The method that we now consider — the SDFEM/SUPG— is designed to deliver improved stability without compromising accuracy in its computed solutions.

Definition of SDFEM/SUPG [12] for (3): find $u^N \in V^N$ such that for all $v \in V^N$,

$$\begin{aligned} a_{SD}(u^N, v^N) &:= \varepsilon(\nabla u^N, \nabla v^N) + (\mathbf{a}\cdot\nabla u^N, v^N) + (cu^N, v^N) \\ &\quad + \sum_{T\in\mathcal{T}_h} \delta_T(\varepsilon\Delta u^N + \mathbf{a}\cdot\nabla u^N + cu^N, \mathbf{a}\cdot\nabla v^N)_T \\ &= (f, v^N) + \sum_{T\in\mathcal{T}_h} \delta_T(f, \mathbf{a}\cdot\nabla v^N)_T, \end{aligned}$$

where $\delta_T \geq 0$ is a user-chosen locally constant parameter (i.e. constant on each mesh element) and $(\cdot,\cdot)_T$ is the $L^2(T)$ inner product. If $\delta_T = 0$ for all T then one obtains the unstable Galerkin method of Figure 8, so we shall certainly set $\delta_T > 0$ for at least some $T \in \mathcal{T}_h$.

Terminology: SDFEM stands for "Streamline Diffusion Finite Element Method" — the method is essentially equivalent to adding a local amount $O(\delta_T)$ of diffusion to (3) but only in the convective direction. This direction is also called the "streamline" direction in the case of a steady-state problem. On the other hand, SUPG is an acronym for "Streamline Upwinding Petrov-Galerkin method": Petrov-Galerkin means that the FEM trial space differs from the test space — one can write the SDFEM/SUPG as a standard Galerkin method with trial space V^N and test space functions $v^N + \mathbf{a}\cdot\nabla v^N$ for all $v^N \in V^N$.

4..1. Stability

Set $c_T = \max_{x\in T} |c(x)|$ for each $T \in \mathcal{T}_h$. Assume that for all those mesh elements $T \in \mathcal{T}_h$ where $\delta_T > 0$, the mesh is quasiuniform with local inverse inequality $\|\Delta v^N\|_{0,T} \leq \mu_{inv} h_T^{-1} |v^N|_{1,T}$ for all T, where $h_T = \ diam(T)$. Here $|\cdot|_{1,T}$ is the seminorm in $H^1(T)$ and $\|\cdot\|_{0,T}$ is the $L^2(T)$ norm. Choose δ_T to satisfy

$$0 \leq \delta_T \leq \frac{1}{2}\min\left(\frac{c_0}{c_T^2}, \frac{h_T^2}{\varepsilon\mu_{inv}^2}\right) \tag{5}$$

for each $T \in \mathcal{T}_h$.

For each $v^N \in V^N$, we have

$$\begin{aligned} a_{SD}(v^N, v^N) &\geq \varepsilon|v^N|_1^2 + c_0\|v^N\|_0^2 + \sum_{T\in\mathcal{T}_h} \delta_T\|\mathbf{a}\cdot\nabla v^N\|_{0,T}^2 \\ &\quad + \sum_{T\in\mathcal{T}_h} \delta_T(-\varepsilon\Delta v^N + cv^N, \mathbf{a}\cdot\nabla v^N)_T\ . \end{aligned}$$

Using the local inverse inequality and the assumption (5),

$$\begin{aligned} &\left|\sum_T \delta_T(-\varepsilon\Delta v^N + cv^N, \mathbf{a}\cdot\nabla v^N)_T\right| \\ &\leq \sum_T \varepsilon^2\delta_T\|\Delta v^N\|_{0,T}^2 + \sum_T c_T^2\delta_T\|v^N\|_{0,T}^2 + \frac{1}{2}\sum_T \delta_T\|\mathbf{a}\cdot\nabla v^N\|_{0,T}^2 \\ &\leq \frac{\varepsilon}{2}|v^N|_1^2 + \frac{c_0}{2}\|v^N\|_0^2 + \frac{1}{2}\sum_T \delta_T\|\mathbf{a}\cdot\nabla v^N\|_{0,T}^2. \end{aligned}$$

Hence the discrete bilinear form is coercive, i.e.

$$a_{SD}(v^N, v^N) \geq \frac{1}{2}|||v^N|||_{SD}^2 \tag{6}$$

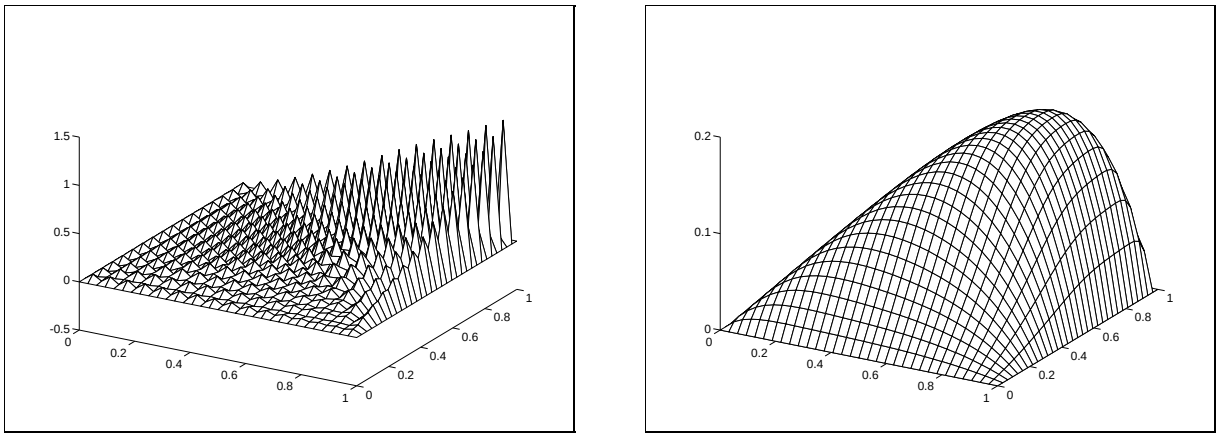

Figure 9: Galerkin FEM and SDFEM solutions computed on uniform meshes, $\varepsilon = 10^{-3}$

for all $v^N \in V^N$. Here

$$|||w|||_{SD} := \Big(\varepsilon|w|_1^2 + \sum_{T\in\mathcal{T}_h} \delta_T \|\mathbf{a}\cdot\nabla w\|_{0,T}^2 + c_0\|w\|_0^2\Big)^{1/2}.$$

The stronger stability of (6), compared with (4), leads us to hope that the SDFEM will compute solutions that are less oscillatory than the standard Galerkin method. This is indeed the case, as Figure 9 demonstrates.

4..2. Convergence results, choice of δ_T

Now that we have a stability bound in (6), we can deduce a preliminary error bound for the computed solution. Write u^I for the usual FEM interpolant to u from V^N. Then

$$\frac{1}{2}|||u^I - u^N|||_{SD}^2 \le a_{SD}(u^I - u^N, u^I - u^N) = a_{SD}(u^I - u, u^I - u^N).$$

Estimating the right-hand side term by term [30], one arrives at

$$|||u^I - u^N|||_{SD} \le Ch^k \Big[\sum_T (\varepsilon + \delta_T + \delta_T^{-1}h_T^2 + h_T^2)|u|_{k+1,T}^2\Big]^{1/2}, \tag{7}$$

where $h = \max_T h_T$ and $|\cdot|_{k+1,T}$ is a local Sobolev seminorm. Define the local Mesh Peclét number

$$(Pe)_T := \frac{h_T\|\mathbf{a}\|_{L^\infty(T)}}{2\varepsilon}.$$

The bound (7) and the assumption (5) that was needed earlier for coercivity together lead to the natural choice

$$\delta_T = \begin{cases} C_0 h_T & \text{if } (Pe)_T > 1, \\ C_1 h_T^2/\varepsilon & \text{if } (Pe)_T \le 1, \end{cases} \tag{8}$$

where C_0 is user-chosen and locally constant. Then since V^N comprises piecewise polynomials of degree k, one gets

$$|||u - u^N|||_{SD} \le C(\varepsilon^{1/2} + h^{1/2})h^k|u|_{k+1} \tag{9}$$

where $|\cdot|_{k+1}$ is the usual seminorm in $H^{k+1}(\Omega)$. While the bound (9) is superficially attractive, it should be borne in mind that typically $|u|_{k+1} = O(\varepsilon^{-k-1/2})$, so in fact the right-hand side of

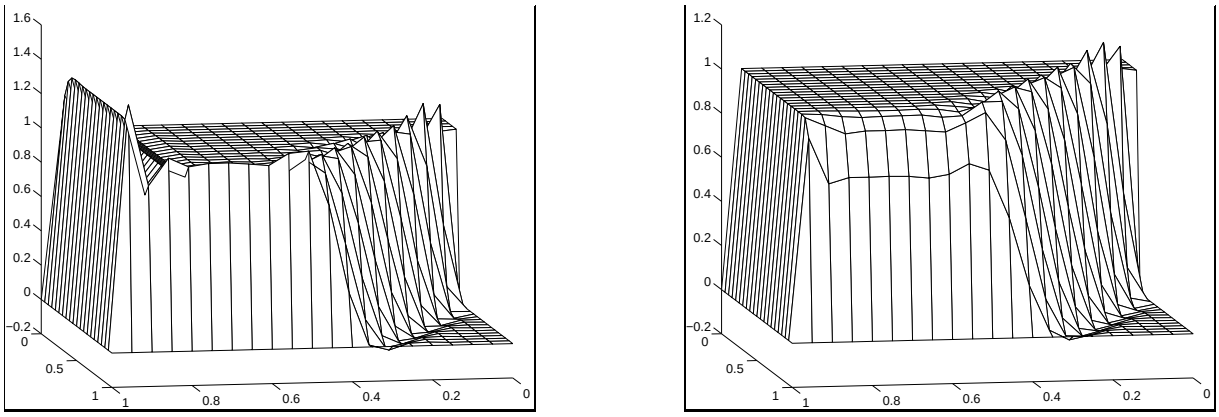

Figure 10: The same problem solved for two values of δ_T

(9) may be very large. Nevertheless one can often localize a result such as (9) to regions away from layers using cut-off functions as in [13, 30].

The same numerical example is solved for two different choices of a globally constant δ_T in Figure 10; the value of δ_T is the left-hand picture is chosen to suit the layer in the foreground, while that of the second picture suits the layer on the left-hand side of the picture.

In general, no precise general formula for an "optimal" (in some sense) value of the SDFEM parameter δ_τ is known; the inequalities seen already seem to be the best general statement that one can make. There has been much research into this question; see, e.g., [1, 2, 8, 9, 11, 26], and the surveys in [30, 31].

4..3. Local error bounds away from layers

For the rest of the paper we consider error bounds for the SDFEM that neither explicitly nor implicitly involve negative powers of ε, unlike (9). First we examine error bounds that hold true only on regions that are sufficiently far from layers. Such bounds are proved using cut-off functions. We do not give a precise definition of these regions and functions but instead refer the reader to [13, 29, 30] for this information.

To begin with, consider L^2-type error bounds. Using cut-off functions one can localize (9) to an error bound away from layers, on a region that we shall write as $\cup\{T : T \in \mathcal{T}_h'\}$ for some subset $\mathcal{T}_h'$ of $\mathcal{T}_h$. Here $|u|_{k+1}$ is of moderate size so the bound does show that the error is small. In particular one then obtains the optimal order of convergence $O(h^k)$ for the *streamline derivative* error

$$\Big(\sum_{T\in\mathcal{T}_h'} \|\mathbf{a}\cdot\nabla(u-u^N)\|_{0,T}^2 \Big)^{1/2},$$

but only $O(h^{k+1/2})$ — half an order less than optimal — for the L^2 error $\left(\sum_{T\in\mathcal{T}_h'} \|u-u^N\|_{0,T}^2\right)^{1/2}$.

For piecewise linears (abusing the notation we indicate this by writing $V^N = P_1$) this L^2 bound is best possible [37]. For piecewise bilinears ($V^N = Q_1$) on rectangular uniform meshes one obtains [35] the optimal estimate $\|u-u^N\|_0 = O(h^2)$, but for $V^N = Q_k$ with $k > 1$, the suboptimal bound $\|u-u^N\|_0 = O(h^{k+1/2})$ seems to be best possible [36].

Local L^∞ error bounds at points x that lie away from layers are derived for $V^N = P_1$ in [13, 29]:

$$|(u-u^N)(x)| \le Ch^{11/8}\ln(1/h).$$

Numerical results show that a pointwise bound of $O(h^{3/2})$ is best possible for piecewise linears [37], but when convection is (nearly) parallel to a rectangular mesh, Zhou and Rannacher [38] get almost $O(h^2)$ away from layers.

4..4. Characteristic interior layers, shock-capturing

Recall that characteristic layers, which lie parallel to the convective direction $\mathbf{a}$ of (3), may be boundary or interior layers. We discuss interior layers here; characteristic boundary layers will be examined in Section 5..

The numerical results of Figure 10 illustrate the unfortunate fact that varying δ_T does not enable one to compute interior layers accurately. This is unsurprising, since the SDFEM essentially works by artificially increasing diffusion in the convective direction, while what is needed to stabilize the computed solution in interior layers is extra diffusion in the *crosswind direction* that is perpendicular to convection.

In [13, 29] crosswind diffusion was artificially increased by adding to the bilinear form $a_{SD}(u^N, v^N)$ a term

$$\delta_c(\mathbf{a}^\perp \cdot \nabla u^N, \mathbf{a}^\perp \cdot \nabla v^N),$$

where $\mathbf{a}^\perp$ is a unit vector perpendicular to $\mathbf{a}$ and

$$\delta_c = \begin{cases} 0 & \text{if } \varepsilon \geq h_T^{3/2}, \\ h_T^{3/2} - \varepsilon & \text{if } \varepsilon < h_T^{3/2}. \end{cases}$$

This modification, whose precise definition is motivated by a theoretical analysis, increases the stability of the basic SDFEM — oscillations in interior layers are reduced — but the layers are smeared.

More recently other authors have found it more fruitful to add crosswind diffusion in a *nonlinear* way, even though the boundary-value problem (3) is linear. This technique is generally called shock-capturing. The representative works [6, 33] and [25] (which proves existence of a discrete solution to the nonlinear numerical method and provides a good general discussion of shock-capturing) have the following basic idea in common: add to $a_{SD}(u^N, v^N)$ the term

$$a_{sc}(u^N, v^N) := \sum_{T \in T^h} (\tau_T D_{sc} \nabla u^N, \nabla v^N)$$

where D_{sc} is a symmetric positive semi-definite matrix function of moderate size, and the user-chosen "limiter function" $\tau_T \geq 0$ restricts shock-capturing to subregions where the residual $Lu^N - f$ is large. See also [3, 4] for existence of a discrete solution and a weak form of the discrete maximum principle that is suitable for nonlinear numerical methods of this type.

For shock-capturing methods in general, reasonable numerical results are attained but local uniqueness of the discrete solution is not proved and the difference between the computed solution and the true solution is not analysed adequately in the literature.

4..5. Quasioptimality

In classical finite element analyses, one is able to show that the computed solution is quasioptimal; for our convection-diffusion problem this would mean that in some norm $\|\cdot\|$ one has

$$\|u - u^N\| \leq C \inf_{v^N \in V^N} \|u - v^N\|,$$

where we recall that a constant C is independent of ε and of the mesh. Only two results of this type are known, and both are recent:

Sangalli [32] considers a 1-dimensional problem with constant coefficients in the differential operator and takes $V^N = P_1$ on an equidistant mesh. He shows that one gets quasioptimality measured in an interpolated norm that is roughly similar to the norm $|||\cdot|||_{SD}$. The analysis required to prove this result is very sophisticated.

Chen and Xu [5] examine a 1-dimensional problem with variable coefficients and take $V^N = P_1$ on an arbitrary mesh. An unusual and critical feature of their analysis is that they take δ_T to be a piecewise quadratic bubble (instead of the usual piecewise constant):

$$\text{for } T = (x_{i-1}, x_i), \quad \text{take } \delta_T(x) = \tilde{\delta}_T(x - x_{i-1})(x_i - x)$$

with δ'_T a user-chosen constant. By elementary arguments one then obtains quasioptimality in the standard $L^\infty(\Omega)$ norm.

It is not straightforward to extend either of these results to the 2-dimensional case.

5. SDFEM and Shishkin meshes for boundary layers

To obtain accurate solutions inside layers, we now apply the SDFEM on Shishkin meshes.

5..1. Exponential layers

First suppose that in (3) one has $\mathbf{a} = (a_1, a_2)$ with $a_1 > 0, a_2 > 0$, and Ω is the unit square. Then the solution u will have exponential layers along $x = 1$ and $y = 1$.

Using N mesh intervals in each coordinate direction, we construct the Shishkin mesh of Figure 5. Where the mesh is coarse — that is, on $(0, 1-\sigma_x) \times (0, 1-\sigma_y)$ — choose the standard δ_T of (8), and otherwise set $\delta_T = 0$ as numerical experiments [23] show that no stabilization is needed on the fine mesh.

We summarize the main convergence results known for this numerical method. In [24], pointwise convergence results for piecewise linears ($V^N = P_1$) are given; these are the best theoretical results available but they are probably not sharp so we do not describe them here. In [23] numerical results for linears and bilinears are given. They show that bilinears ($V^N = Q_1$) are more accurate in the layer regions. In [35], it is proved that for bilinears one gets

$$|||u^N - u^I|||_{SD} + \|u^N - u\|_{L^2} \le C\varepsilon N^{-3/2} + CN^{-2}\ln^2 N, \tag{10}$$

where u^I is the the nodal interpolant. When $\varepsilon \le N^{-1/2}$ one gets the bound $CN^{-2}\ln^2 N$ here, which can be shown to be optimal. But for $V^N = Q_k$ with $k > 1$, this optimality is lost: the best result attainable seems to be

$$|||u^N - I_N u|||_{SD} + \|u^N - u\|_{L^2} \le CN^{-(k+1/2)},$$

where now $I_N u$ denotes Lin's vertices-edges-regions approximant [20], which generalizes the nodal interpolant that was used in the Q_1 result (10).

5..2. Characteristic boundary layers

Consider the problem

$$-\varepsilon\Delta u - a_1 u_x = f \text{ on } \Omega = (0,1)^2, \qquad u = 0 \text{ on } \partial\Omega, \tag{11}$$

with $a_1 > 0$ on $\bar{\Omega}$. The solution u typically has an exponential boundary layer at $x = 0$ and characteristic boundary layers at $y = 0, 1$.

A question that has puzzled researchers for many years is: what is the best choice for the SDFEM parameter δ inside characteristic boundary layers? Numerical and theoretical results [17] show that if one takes $\delta_T = \delta$ for all T when solving the above problem, then for piecewise linears and bilinears the SDFEM is at best $O(\delta)$ pointwise accurate inside characteristic boundary (and interior) layers, *even on Shishkin meshes*. This is disappointing since a standard SDFEM analysis like that leading to (9) motivates the choice $\delta = O(N^{-1})$ inside the parabolic layer (here the mesh has N intervals in each coordinate direction) — so the best we can then hope for is first-order pointwise convergence despite the combination of a good numerical method with a good mesh.

Use the Shishkin mesh of Figure 6, which we reproduce in Figure 11 together with subregions Ω_{ij} corresponding to the different mesh subdomains.

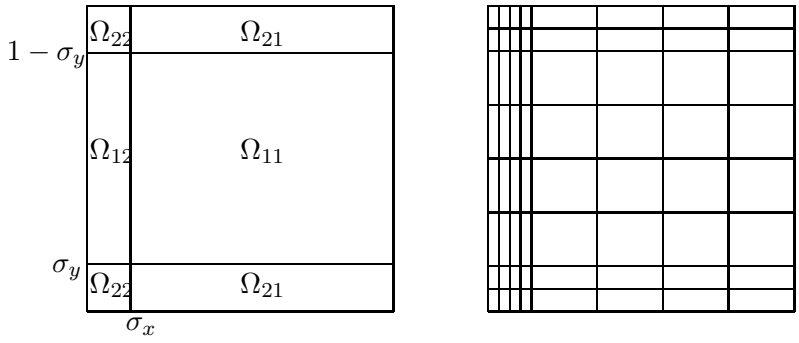

Figure 11: Regions in Shiskin mesh with one exponential and two parabolic layers

The first successful analysis of the SDFEM using piecewise bilinears on such a mesh appears in the recent papers [9, 10]: writing δ_{ij} for the value of δ_T used on the region Ω_{ij} in Figure 11, choose

$$\begin{aligned} \text{(away from layers) } \delta_{11} &= C \min\{N^{-1},\ \varepsilon^{-1}N^{-2}\}, \\ \text{(exponential outflow layer) } \delta_{12} &= C\varepsilon N^{-2}, \\ \text{(corner layers) } \delta_{22} &= C\varepsilon^{3/4}N^{-2}, \\ \text{(characteristic boundary layers) } \delta_{21} &= C\varepsilon^{-1/4}N^{-2}. \end{aligned}$$

Then with u^I the piecewise bilinear nodal interpolant, we have [9, 10]

$$\|u^I - u^N\|_{SD} \leq CN^{-2}\ln^2 N; \tag{12}$$

this order of convergence is optimal up to the $\ln N$ factor.

The bound (12) is proved under the assumption that the solution u of (11) can be decomposed into a sum of the form (2) where the constituent terms are known to have certain plausible properties. This assumption is justified in [15, 14], where it is shown that it suffices to have sufficient smoothness of a_1 and f together with the corner compatibility conditions $f(0,0) = f(1,0) = f(1,1) = f(0,1) = 0$.

5..3. Conclusions

Our current understanding of the SDFEM can be briefly summarized as follows:

- its behaviour and analysis are fairly well understood in boundary layers (both exponential and characteristic);
- but interior layers are still not completely tamed.

Acknowledgements: Most figures in this article were supplied by Niall Madden and Torsten Linß, for whose generous help I am grateful.

References

[1] J. E. Akin and T. E. Tezduyar. Calculation of the advective limit of the SUPG stabilization parameter for linear and higher-order elements. *Comput. Methods Appl. Mech. Engrg.*, 193:1909–1922, 2004.

[2] F. Brezzi and A. Russo. Choosing bubbles for advection-diffusion problems. *Math. Models Methods Appl. Sci.*, 4:571–587, 1994.

[3] E. Burman and A. Ern. Nonlinear diffusion and discrete maximum principle for stabilized Galerkin approximations of the convection–diffusion-reaction equation. *Comput. Methods Appl. Mech. Engrg.*, 191:3833–3855, 2002.

[4] E. Burman and A. Ern. Stabilized Galerkin approximation of convection-diffusion-reaction equations: discrete maximum principle and convergence. *Math. Comp.*, 74:1637–1652 (electronic), 2005.

[5] L. Chen and J. Xu. An optimal streamline diffusion finite element method for a singularly perturbed problem. In Z.C Shi, Z. Chen, T. Tang, and D. Yu, editors, *Recent Advances in Adaptive Computation*, volume 383 of *Contemporary Mathematics*, pages 236–246. American Mathematical Society, 2005.

[6] R. Codina. *A finite element formulation for the numerical solution of the convection-diffusion equation*, volume 14 of *Monograph Series*. Centro Internacional de Métodos Numéricos en Ingeniería, Barcelona, 1993.

[7] P.A. Farrell, A.F. Hegarty, J.J. Miller, E. O'Riordan, and G.I. Shishkin. *Robust Computational Techniques for Boundary Layers*. Chapman & Hall/CRC, Boca Raton, 2000.

[8] B. Fischer, A. Ramage, D. J. Silvester, and A. J. Wathen. On parameter choice and iterative convergence for stabilised discretisations of advection-diffusion problems. *Comput. Methods Appl. Mech. Engrg.*, 179:179–195, 1999.

[9] S. Franz and T. Linß. Superconvergence analysis of Galerkin FEM and SDFEM for elliptic problems with characteristic layers. Technical Report MATH-NM-03-2006, Institut für Numerische Mathematik, Technische Universität Dresden, 2006.

[10] S. Franz, T. Linß, and H.-G. Roos. Superconvergence analysis of the SDFEM for elliptic problems with characteristic layers. (Submitted for publication).

[11] P. Houston and E. Süli. Stabilised *hp*-finite element approximation of partial differential equations with nonnegative characteristic form. *Computing*, 66:99–119, 2001.

[12] T.J.R. Hughes and A.N. Brooks. A multidimensional upwind scheme with no crosswind diffusion. In T.J.R. Hughes, editor, *Finite Element Methods for Convection Dominated Flows*, volume 34 of *AMD*. ASME, New York, 1979.

[13] C. Johnson, A. H. Schatz, and L. B. Wahlbin. Crosswind smear and pointwise errors in streamline diffusion finite element methods. *Math. Comp.*, 49:25–38, 1987.

[14] R.B. Kellogg and M. Stynes. Sharpened bounds for corner singularities and boundary layers in a simple convection-diffusion problem. (Submitted for poublication).

[15] R.B. Kellogg and M. Stynes. Corner singularities and boundary layers in a simple convection-diffusion problem. *J. Differential Equations*, 213:81–120, 2005.

[16] P. Knobloch and L. Tobiska. The P_1^{mod} element: a new nonconforming finite element for convection-diffusion problems. *SIAM J. Numer. Anal.*, 41:436–456 (electronic), 2003.

[17] N. Kopteva. How accurate is the streamline-diffusion FEM inside characteristic (boundary and interior) layers? *Comput. Methods Appl. Mech. Engrg.*, 193:4875–4889, 2004.

[18] N. Kopteva. Maximum norm error analysis of a 2d singularly perturbed semilinear reaction-diffusion problem. *Math. Comp.*, to appear.

[19] K.A. Lemke. Illustrated glossary of alpine glacial landforms. In *The Virtual Geography Department Project*. University of Wisconsin–Stevens Point, www.uwsp.edu/geo/faculty/lemke/alpine_glacial_glossary.

[20] Q. Lin. A rectangle test for interpolated finite elements. In *Proc. Syst. Sci. Eng.*, pages 217–229. Great Wall (H.K.) Culture Publish Co., 1991.

[21] T. Linß. Layer-adapted meshes for convection-diffusion problems. *Comput. Methods Appl. Mech. Engrg.*, 192:1061–1105, 2003.

[22] T. Linß. *Layer-adapted meshes for convection-diffusion problems*. Habilitationsschrift, Technische Universität Dresden, Germany, 2006.

[23] T. Linß and M. Stynes. Numerical methods on Shishkin meshes for linear convection-diffusion problems. *Comput. Methods Appl. Mech. Engrg.*, 190:3527–3542, 2001.

[24] T. Linß and M. Stynes. The SDFEM on Shishkin meshes for linear convection-diffusion problems. *Numer. Math.*, 87:457–484, 2001.

[25] G. Lube and G. Rapin. Residual-based stabilized higher-order fem for advection-dominated problems. *Comput. Methods Appl. Mech. Engrg.*, 195:4124–4138, 2006.

[26] N. Madden and M. Stynes. Efficient generation of oriented meshes for solving convection-diffusion problems. *Int. J. Numer. Methods Engrg.*, 40:565–576, 1997.

[27] J.J.H. Miller, E. O'Riordan, and G.I. Shishkin. *Solution of singularly perturbed problems with ε-uniform numerical methods—introduction to the theory of linear problems in one and two dimensions*. World Scientific, Singapore, 1996.

[28] K.W. Morton. *Numerical solution of convection-diffusion problems*. Chapman & Hall, London, 1996.

[29] K. Niijima. Pointwise error estimates for a streamline diffusion finite element scheme. *Numer. Math.*, 56:707–719, 1990.

[30] H.-G. Roos, M. Stynes, and L. Tobiska. *Numerical methods for singularly perturbed differential equations*, volume 24 of *Springer Series in Computational Mathematics*. Springer-Verlag, Berlin, 1996.

[31] H.-G. Roos, M. Stynes, and L. Tobiska. *Numerical methods for singularly perturbed differential equations*. Springer Series in Computational Mathematics. Springer-Verlag, Berlin, Second edition, (to appear).

[32] G. Sangalli. Quasi-optimality of the SUPG method for the one-dimensional advection-diffusion problem. *SIAM J. Numer. Anal.*, 41:1528–1542 (electronic), 2003.

[33] Y.-T. Shih and H.C. Elman. Iterative methods for stabilized discrete convection-diffusion problems. *IMA J. Numer. Anal.*, 20:333–358, 2000.

[34] M. Stynes. Steady-state convection-diffusion problems. *Acta Numer.*, 14:445–508, 2005.

[35] M. Stynes and L. Tobiska. The SDFEM for a convection-diffusion problem with a boundary layer: optimal error analysis and enhancement of accuracy. *SIAM J. Numer. Anal.*, 41:1620–1642, 2003.

[36] M. Stynes and L. Tobiska. Using rectangular Q_p elements in the SDFEM for a convection-diffusion problem with a boundary layer. Technical Report 08-2006, Faculty of Mathematics, Otto-von-Guericke-Universität, Magdeburg, 2006.

[37] G. Zhou. How accurate is the streamline diffusion finite element method? *Math. Comp.*, 66:31–44, 1997.

[38] G. Zhou and R. Rannacher. Pointwise superconvergence of the streamline diffusion finite-element method. *Numer. Methods Partial Differential Equations*, 12:123–145, 1996.